AMORPHOUS SURFACE LAYERS IN Ti-IMPLANTED Fe*

CONF 791112--36

J.A. Knapp, D.M. Follstaedt, and S.T. Picraux
Sandia Laboratories†
Albuquerque, New Mexico

We observe that implanting Ti into high-purity Fe results in an amorphous surface layer which is composed of not only Fe and Ti, but also C. Implantations were carried out at room temperature over the energy range 90-190 keV and fluence range 1 - 20 x 10^{16} at/cm^2. The Ti-implanted Fe system has been characterized using transmission electron microscopy (TEM), ion backscattering and channeling analysis, and (d,p) nuclear reaction analysis. The amorphous layer was observed to form at the surface and grow inward with increasing Ti fluence. For an implant of 1 x 10^{17} Ti/cm^2 at 180 keV the layer thickness was 150 Å, while the measured range of the implanted Ti was ~550 Å. This difference is due to the incorporation of C into the amorphous alloy by C being deposited on the surface during implantation and subsequently diffusing into the solid. Our results indicate that C is an essential constituent of the amorphous phase for Ti concentrations $\lesssim$10 at.%. For the 1 x 10^{17} Ti/cm^2 implant, the concentration of C in the amorphous phase was ~25 at.%, while that of Ti was only ~3 at.%. A higher fluence implant of 2 x 10^{17} Ti/cm^2 produced an amorphous layer with a lower C concentration of ~10 at.% and a Ti concentration of ~20 at.%.

---

*This work supported by the U.S. Department of Energy, DOE, under Contract DE-AC04-76-DP00789.

†A U.S. Department of Energy Facility.

Introduction

Amorphous metallic alloys show considerable promise in reducing wear or corrosion in a variety of systems(1). By ion implantation such amorphous alloys can be formed independently of bulk properties. Thus far, implantation-produced amorphous alloys have been described as binary systems consisting of a single species implanted into the host material. We report here the observation of a surface amorphous alloy on Fe which incorporates not only implanted Ti, but also C which is brought in from the surface during the implantation process. We have studied this alloy using both TEM analysis and ion beam analysis and have concluded that the C is an essential constituent, at least at Ti concentrations <10 at.%. Our results are the first to demonstrate that implanted amorphous alloys can be ternary because of the introduction of impurities such as C at the surface.

Experimental Procedures

A disk approximately 10 mm diameter and 2 mm thick with the face perpendicular to the <100> axis was spark-cut from an iron single crystal rod of 99.99% purity. It was electropolished in a solution of 450 ml methanol, 50 ml distilled water, and 50 ml concentrated nitric acid at ~ -60°C to remove ~ 0.1 mm of possibly spark-damaged material from each side and to produce a mirror finish. For TEM studies, iron foil of 50 μm thickness and the same purity was cut to convenient sizes for implantation (~1 cm x 2 cm), degreased, and then annealed overnight in high vacuum (~ 10^{-7} torr) at 860°C to produce large grain (~ 100μm), damage free polycrystalline foils. These were electropolished to a mirror finish with the above procedure.

An implanter fitted with a sputtering source(2) was used to implant Ti^+. Prior to implantation, the sample chamber was pumped to ~ 3×10^{-7} torr with a turbo-molecular pump. During implantation the pressure rose to ~ 3×10^{-6} torr. Residual gas analysis has shown that the increased pressure is largely due to argon which is used as a carrier gas in the sputtering source. The foils were implanted with a typical flux of ~ 5×10^{12} Ti/cm^2-s to their final fluence and then used for TEM examination. The single crystal was implanted to low fluences, examined with ion beam analysis, and then implanted again to be analyzed at progressively higher fluences.

A single-jet electropolish unit was used to thin the foil samples from the unimplanted side to produce electron-transparent areas. The above solution was used with the following conditions for optimum transparent material. The electrolyte temperature was held between -65 to -73°C. A 1 mm diameter jet was used with a separation of 5 mm between the nozzle and the sample. A voltage of 220 V was used to obtain a current of 15 mA. The electrolyte flow rate was as slow as possible consistent with a stable jet and with removal of bubbles forming on the sample during polishing. Following automatic shutoff of the jet when light was detected passing through the sample by a detector beneath it, the sample was rinsed (about 1 minute in each rinse) twice in absolute ethanol, once in acetic acid (25 ml) diluted with methanol (450 ml), followed by pure methanol and finally absolute ethanol.

We have presented these details because this procedure had the fortunate effect of not attacking the amorphous layer. The electropolish removed the crystalline material, but left large areas of the amorphous layer exposed. An example is shown in Fig. 1. From the high transparency the layer's thickness is estimated to be $\lesssim$ 500 Å. Normally, an electropolished TEM sample is penetrated and the material around the edge of the resulting hole is studied. It is then difficult to find large areas of very thin sample so

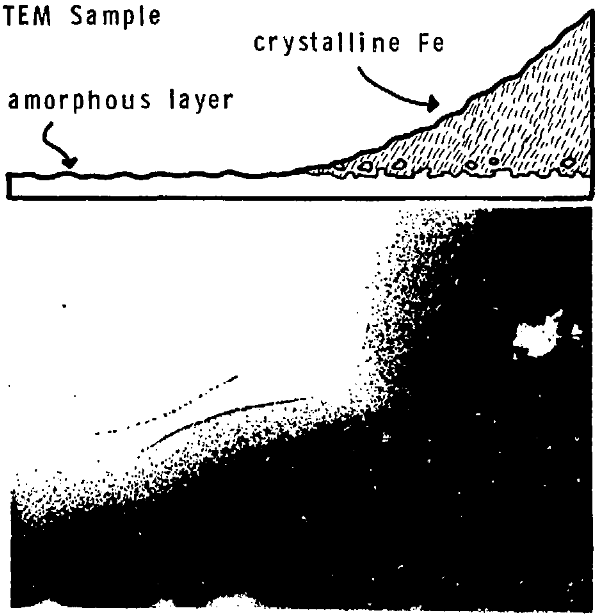

Fig. 1 - Bright field TEM micrograph of Fe implanted with 2×10^{17} Ti/cm^2 showing the very transparent, thin amorphous layer (white area). Shown just above the micrograph is an illustration of the sample cross section after thinning.

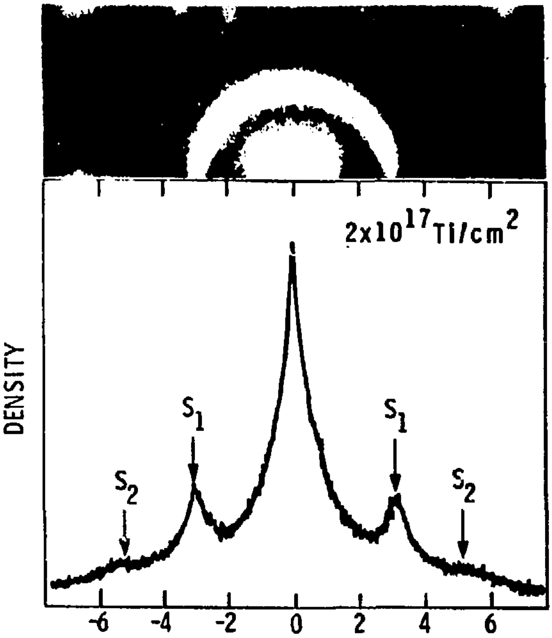

Fig. 2 - Electron Diffraction pattern from the thin amorphous layer in Fe implanted with 2×10^{17} Ti/cm^2, and its microdensitometer trace.

that material very near the implanted surface can be observed alone. However, with these samples, the amorphous layer could be observed without the superimposed image of the underlying crystalline material. This also allowed selected area diffraction patterns to be obtained from the amorphous layer without the superimposed reflections of underlying material. Examining progressively thicker sections of the sample allows depth information to be obtained from the TEM projected images.

Ion backscattering and nuclear reaction profiling data were obtained using a Van de Graaff ion accelerator. Depth profiling of the disordered regions in the implanted Fe crystal was done by channeling 1.8 MeV ^{4}He ions along the <100> axis. Deuterium ions at several different energies were used to identify the levels of C and O present in the sample through (d,p) nuclear reactions(3). The concentration profile of the Ti implants was determined using 6 MeV ^{4}He ion backscattering.

Transmission Electron Microscope Results

Three implantation conditions were examined with TEM: 4×10^{16} Ti/cm^2 implanted at 180 keV, 1×10^{17} Ti/cm^2 at 180 keV, and 2×10^{17} Ti/cm^2 with the implant energy varied from 190-90 keV in 4 nearly equal steps. The highest fluence offered conclusive evidence of an amorphous surface layer. A diffraction pattern obtained from the thin layer and its microdensitometer trace are shown in Fig. 2. The two diffuse rings have wave numbers ($S = 4\pi/\sin\theta = 2\pi/d$, where d is the atomic spacing) $S_1 = 3.06$ Å^{-1} and $S_2 = 5.29$ Å^{-1} which are typical of other amorphous Fe systems(4). The diffuse ring pattern is not that of iron oxides; samples which have oxidized show a diffuse ring closer to the undeflected beam. The diffraction pattern shows very little evidence of crystalline Fe in the center of the very transparent area.

The 4×10^{16} Ti/cm^2 sample showed similar very transparent regions. Electron diffraction patterns from these areas show the same amorphous rings plus an oriented Fe diffraction pattern. The latter is due to Fe crystallites

Fig. 3 - Dark field micrograph using a {110} Fe reflection to illuminate Fe crystallites embedded in the very transparent amorphous layer in Fe implanted with 4×10^{16} Ti/cm^2.

embedded in the amorphous material as shown in Fig. 3. The pattern orientation is the same as that of the thicker, crystalline regions of the sample immediately surrounding the very transparent area, and the crystallites exhibit the same contrast as the surrounding material. We conclude that the amorphous, transparent layer contains iron crystallites embedded in it which retain the orientation of the original large grain. The transparent layer does not, however, contain all the implanted Ti as evidenced by a dense array of dislocations created as the Ti ions come to rest in the thicker crystalline sample regions.

The 1 x 10^{17} Ti/cm^2 foil had similar very transparent areas which showed less crystalline Fe than observed at 4 x 10^{16} Ti/cm^2. Thicker sample regions also showed dense dislocation arrays, again demonstrating that the amorphous layer does not extend to the full depth of the Ti range. Thus, TEM shows that a thin layer on the surface of the Ti-implanted Fe is amorphous, with oriented crystalline Fe embedded in it. The amount of oriented Fe decreases with increasing Ti fluence.

Channeling and Nuclear Reaction Results

In order to systematically study the formation of the amorphous regions in Fe, depth profiles of disordered Fe were obtained using 1.8 MeV ^{4}He channeling along the <100> direction, with glancing emission angle detection. Four channeling spectra are shown in Fig. 4 for Ti fluences ranging from 1 x 10^{16} to 2 x 10^{17} atoms/cm^2, where the depth has been obtained assuming the density and electronic stopping power of pure Fe. A random spectrum is also shown for each Ti fluence. The shapes of the random spectra are modified by two factors as the fluence is increased. First, the atomic percentage of Fe in the implanted region is reduced, which reduces the height of the random

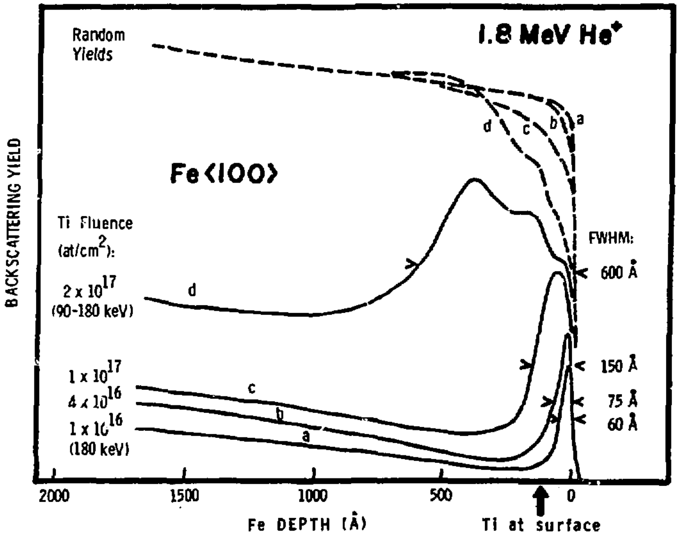

Fig. 4 - Helium channeling spectra obtained along the Fe <100> axis for several fluences of implanted Ti.

spectra. Second, direct scattering from Ti atoms overlaps the Fe scattering, beginning at the energy corresponding to the surface Ti, marked on the depth scale of Fig. 4. This Ti signal increases the random spectra, counteracting the loss of Fe signal. It should be noted that the Ti signal can also be a component of the channeled spectra at depths below the Ti mark.

The channeling spectra are characterized by a peak at the surface which grows in height (a measure of disorder) and depth as the Ti fluence is increased. At the lowest fluence (1×10^{16}), the disorder peak is ~ 2 times as high as the surface peak from a virgin cyrstal (not shown) and 60 Å full width at half-maximum. This width increases to 150 Å as the Ti fluence is increased to 1×10^{17} Ti/cm^2. The range of Ti implanted at 180 keV was determined separately by 6 MeV ion backscattering to be ~ 550 Å, with $\Delta R \simeq 300$ Å. Thus, for $1 - 10 \times 10^{16}$ Ti/cm^2 implanted at 180 keV, the disordered region at the surface is much shallower than the depth profile of the implanted Ti. Only in the heaviest implant of 2×10^{17} Ti/cm^2 does the depth of the disordered region approach the range of the implant. This was a multiple energy implant (90 - 180 keV) which brought the Ti concentration in the first 400 - 500 Å up to ~ 20 at.%.

In light of the TEM results previously discussed, the disorder peaks in the spectra of Fig. 4 are interpreted as being associated with a partially amorphous region, rather than to the presence of precipitates. This amorphous region is seen to grow inward from the surface as a function of Ti fluence. The height of the disorder peak relative to the random yield for each fluence is then a measure of the percentage of amorphous material at that depth. The fact that some He$^+$ ions are being channeled through the amorphous layer requires that crystalline Fe be present at the same depth and that it have the same orientation as the underlying bulk of the single crystal. As the Ti fluence is increased, the crystalline fraction is reduced, as seen by the increasingly higher yields, until at 2×10^{17} Ti/cm^2 the surface region is nearly totally amorphous. Thus, the channeling and TEM are complementary and both give the same microstructure for the near surface amorphous layer.

The channeling results clearly show that the amorphous region appears at the surface and grows inward, rather than conforming to the Ti profile or the damage that the Ti introduces. This involvement of the surface suggests that impurities present at the surface might be introduced by the incident Ti ions to produce the amorphous region. The primary surface contaminants are C and O; thus to test this possibility, the levels of C and O present in the sample were determined by (d,p) nuclear reaction analysis. The results showed very significant levels of C present which increased with increasing Ti fluence, whereas the levels of O contamination were negligible ($\lesssim 7 \times 10^{15}$ at./cm^2) and did not increase with Ti fluence. Measured levels of total C vs. total implanted Ti ranged from 1:3 to 1:1 depending on the implantation history of the sample. The local concentrations of C and Ti in the amorphous phase can be obtained with the assumption that all the C is in the amorphous material and that the Ti within the amorphous thickness is divided proportionately between amorphous and crystalline Fe. These estimated concentrations are ~ 3 at.% Ti and ~ 25 at.% C for the 1×10^{17} at./cm^2 implant, and ~ 20 at.% Ti and ~ 10 at.% C for the 2×10^{17} at./cm^2 implant.

Carbon Introduction by Ti Implantation

We consider two methods by which C can be introduced into the Fe(Ti) substrate. The C content of the near surface as a function of Ti fluence (Table I) can be fit with a linear increase and a non-zero intercept. We interpret this relation as follows. A carbon layer is formed on the sample surface during Ti implantation. This is commonly observed during implantation and is thought to be due to a breakdown of residual hydrocarbon molecules by the ion beam. We assume that during implantation a steady-state amount of C is reached after achieving a minimum Ti fluence ($\lesssim 4 \times 10^{16}$ Ti/cm^2). With increasing Ti fluence, additional C is incorporated into the sample while the surface C content remains essentially constant. An estimate of the surface C is then obtained from the zero fluence intercept, $\sim 2 \times 10^{16}$ C/cm^2.

Kelley and Sanders(5) have examined recoil implantation of a layer of surface ions during implantation. They have evaluated the quantity $H/I\theta$ for oxygen on several substrates being bombarded with ions covering a wide mass range (He, Ne, and Xe). H is the number of O atoms driven deeper than 5 Å into the substrate for each incident ion when the surface coverage is one monolayer. I is the incident ion fluence and θ the surface coverage as a fraction of a monolayer. H increases roughly linearly with the incident ion mass, and we have scaled their results to Ti. At their highest energy (100 keV), the results become approximately substrate independent (to within $\sim \pm 10\%$) for Be, Aℓ, and Mo, and we therefore apply them to Fe. Extrapolating to 180 keV gives $H/I\theta = 0.01$ to 0.02. Taking this value for C and setting $\theta \sim 1$, 10^{17} Ti/cm^2 at 180 keV should then recoil implant $\sim 2 \times 10^{15}$ C/cm^2. This is far lower than our observed C content ($\sim 5 \times 10^{16}$ C/cm^2). Their work was done for $0 < \theta \lesssim 1$, and while we expect some increase in implanted C since our coverage is ~ 10 monolayers, this increase would probably be less than tenfold, and in any event, appreciably smaller than the observed C levels. Thus, recoil implantation does not appear to be responsible for the C introduction into our amorphous layer.

A second method we consider is C diffusion from the surface layer into the substrate during implantation. Thermocouple measurements indicate that our samples reach 40 – 50°C during implantation, for which the C diffusivity in Fe is $D = 2 \times 10^{-16}$ cm^2/s(6). Cascade mixing can also be regarded as a diffusion process(7,8), but calculations yield a significantly smaller effective diffusivity ($\sim 1 \times 10^{-17}$ cm^2/s). Assuming that a constant source of C is maintained at the surface during implantation, the amount of C which can diffuse into the substrate is given by(9)

$$L(T) = c_0 N \sqrt{\frac{4Dt}{\pi}} \quad , \tag{1}$$

where c_0 is the effective solubility level for C in our Fe(Ti). From the C content of the amorphous layer and its thickness, we estimate $c_0 \sim 0.3$. In Table I we have listed the Ti implantations studied and the observed C contents and also the calculated values for L and $\sqrt{Dt}$ using $D = 2 \times 10^{-16}$ cm^2/s. Here t is taken to be the implant time since that is the time over which the C surface source is maintained. Diffusion appears able to incorporate the amount of C we observe and to account for the amorphous layer depth, with the possible exception of the highest fluence. The latter implant had a higher local concentration of Ti which may have permitted formation of the amorphous phase at deeper depths. While we cannot rule out contributions from recoil implantation, C diffusion from a surface source appears better able to account for the C in our amorphous layers. Also, no enhancement in the C diffusion rate during implantation is required to explain the observed results. For a constant Ti flux, Equation (1) predicts a square root dependence of C on implanted Ti, which is also allowed by the C accumulation results.

TABLE I

Ti Fluence	Implant Time	Observed C Content	Estimated C Content	Amorphous Thickness	$\sqrt{Dt}$
(at./cm^2)	(hr.)	(at./cm^2)	(at./cm^2)	(Å)	(Å)
1×10^{16}	~ 0.5		1.7×10^{16}	60	60
4×10^{16}	~ 2	3.2×10^{16}	3.4×10^{16}	75	120
1×10^{17}	~ 6		6.0×10^{16}	150	210
2×10^{17}	~12	6.8×10^{16}	8.5×10^{16}	600	290

Discussion

We have observed that implanted Ti into Fe forms an amorphous layer at the surface which incorporates not only Ti and Fe, but also C. Implanted Ti by itself into Fe does not form an amorphous alloy for concentrations up to to ~ 10 at.%. This is shown by the fact that the amorphous thickness for 1×10^{17} Ti/cm^2 at 180 keV is much less than the Ti range. An illustration of the observed microstructure for the latter implant is shown in Fig. 5. The Ti range and its associated ion damage extend much deeper than the observed amorphous layer. The diffusion model for C introduction from the surface is consistent with this interpretation. For this and the lower fluence implants, the amorphous region is observed to be two-phase, containing both amorphous and crystalline Fe. In the 2×10^{17} Ti/cm^2 implant, the peak Ti concentration is ~ 20 at.%. Since the amorphous layer thickness in this alloy extends to about the Ti range, it is possible that such Ti concentrations could produce amorphous Fe without C.

As a check on whether C by itself in implanted Fe produces an amorphous alloy, we have examined an Fe foil implanted with 1×10^{17} C/cm^2 at 80 keV with electron diffraction. No diffuse rings were observed in the electron

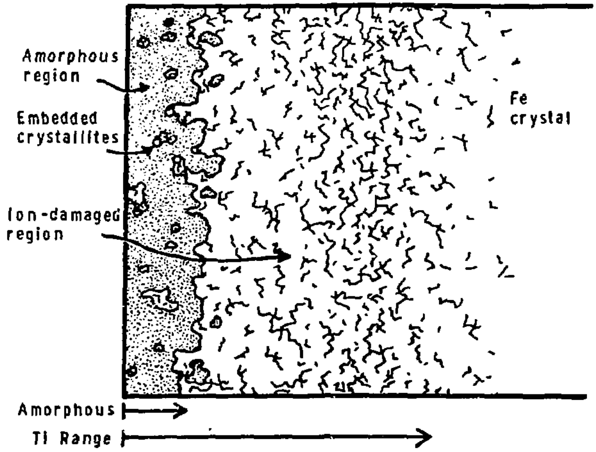

Fig. 5 - Schematic illustration of the observed microstructure for 1×10^{17} Ti/cm^2 implanted into Fe.

diffraction patterns. Vogel(10) has used electron diffraction to study C-implanted Fe and has identified the resulting alloy as (crystalline) martensite. Finally, Fe implantation into Fe, which should form surface C in the same manner as Ti, is reported not to produce an amorphous alloy(11). Thus, C alone in implanted Fe does not appear to produce an amorphous alloy. We conclude that both Ti and C incorporated into implanted Fe are needed to produce an amorphous alloy for Ti concentrations $\lesssim$ 10 at.%. To further elucidate the role of C, experiments in which C is also implanted are in progress.

Previous studies of amorphous alloys(4,11-13) formed by implantation have considered only the host and implanted species as alloy constituents. Our results suggest that C incorporation should be examined in other systems as well. For example, Ta-implanted Fe has been reported to become amorphous above $\sim$ 10 at.% Ta(14). Considering the chemical similarity of Ti and Ta (both are strong carbide formers), the Ta alloy should be examined for surface-introduced C.

Our work is also unique in that we have been able to observe the amorphous layer separately from the crystalline substrate. This allows us to better obtain depth information with TEM by examining progressively thicker sample sections. In addition, it allowed us to observe that at the lower fluences, the "amorphous" layer is actually a two-phase layer containing crystalline Fe as well. Previous implantation studies have not demonstrated such a two phase intermediate step in going from a purely crystalline to a purely amorphous surface layer.

Ion implantation has been shown to favorably alter the surface properties of metals in many instances. In particular, Ti implantation into stainless steels has been shown to reduce the wear rate(15) by a factor of $\sim$ 10. Since improved wear characteristics are observed for amorphous metals, our observed amorphous surface layer may be responsible for the improvement with Ti implantation. The resistance to the very aggressive electropolish environment demonstrates the corrosion resistance of the amorphous layer, and this system may prove important for that property as well.

Acknowledgement

We would like to acknowledge the able assistance of C. T. Fuller and J. M. McDonald with the implantations and the TEM sample preparation. We thank B. L. Doyle for his assistance with the 6 MeV backscattering.

References

1. J. J. Gilman, "Ferrous Metallic Glasses," Metal Progress, 42 (July, 1979).

2. C. T. Fuller, "A Sputtered-Ion Source for the Lintott Ion Accelerator," Sandia Laboratories Report No. SAND76-0040 (1976).

3. J. A. Borders and J. M. Harris, "The Use of $^{12}C(d,p)^{13}C$ and $^{16}O(d,p)^{17}O$ Reactions to Profile Carbon and Oxygen In Solids," Nucl. Inst. and Methods <u>149</u>, 279 (1978).

4. A. Ali, W. A. Grant, and P. J. Grundy, "A Microstructural Study of Some Amorphous Transition Metal-Metalloid Surface Alloys Formed by Ion Implantation," Phil. Mag. B <u>37</u>, 353 (1978).

5. R. Kelley and J. B. Sanders, "Recoil Implantation from a Thin Source, I. Underlying Theory and Numerical Results," Surf. Sci. 57, 143 (1976).

6. J. R. G. da Silva and R. B. McLellan, "Diffusion of Carbon and Nitrogen in B. C. C. Iron," Mat. Sci. and Engr. 26, 83 (1976).

7. H. H. Anderson, "The Depth Resolution of Sputter Profiling," Appl. Phys. (Germany) 18, 131 (1979).

8. S. M. Myers, "Ion-Beam Induced Migration and Its Effect on Concentration Profiles," presented at the Fourth International Conference on Ion Beam Analysis (Aarhus, June 25-29, 1979) (to be published in Nucl. Inst. and Methods).

9. S. M. Myers and J. E. Smugeresky, "Phase Equilibria and Diffusion in the Be-Aℓ-Fe System Using High Energy Ion Beams," Met. Trans. A 7, 755 (1976).

10. F. L. Vogel, Jr., "Implantation of Carbon into Thin Iron Films," Thin Solid Films 27, 369 (1975).

11. W. [illegible] Grant, "Amorphous Metals and Ion Implantation," J. Vac, Sci. Technol. 15, 1644 (1978).

12. J. M. Poate, "Metastable Alloy Formation," J. Vac. Sci. Technol. 15, 1636 (1978).

13. J. A. Borders, "Metastable Phases in Metals Produced by Ion Implantation," Ann. Rev. Mater. Sci., 9, 313 (1979).

14. J. K. Hirvonen, A. G. Cullis, and J. M. Poate, reported in reference 12.

15. J. K. Hirvonen, J. W. Butler, T. P. Smith, R. A. Kant, and V. C. Westcott, "Sliding Wear Reduction by Ion Implantation," presented at the International Conference on Ion Beam Modification of Materials (Budapest, Sept. 4-8, 1978) (to be published in Radiation Effects).